Electronic supplementary information (ESI) for *In-situ* Raman spectroscopic-based microfluidic "lab-on-a-chip" platform for non-destructive and continuous characterization of *Pseudomonas aeruginosa* biofilms

Jinsong Feng, César de la Fuente-Núñez, Michael J. Trimble, Jie Xu, Robert E. W. Hancock, Xiaonan Lu*

Materials and methods

Bacterial strains and growth conditions.

P. aeruginosa PAO1 was cultured in tryptic soy broth (TSB) at 37°C and used throughout the study.

Fabrication of microfluidic "lab-on-a-chip" platform.

Poly-dimethylsiloxane (PDMS) based microfluidic system was fabricated in the Advanced Materials and Process Engineering Lab at UBC using classic soft lithography technique [1]. The microfluidic platform consists of a glass substrate and a PDMS layer. The PDMS layer consists of in/outlet of channels with cultivation chambers. The dimensions of in/outlet were 400 μm (width) × 40 μm (height). The microchamber for biofilm cultivation was designed as a circle shape with dimensions of 300 μm (radius) × 50 μm (height). PDMS layer was bonded to glass slide by oxygen plasma treatment. The microfluidic device was connected to a synergy pump using tubings.

Biofilm formation in the microfluidic "lab-on-a-chip" system.

Overnight cultures of *P. aeruginosa* PAO1 were diluted to a concentration of ~10^7 CFU/ml and introduced into the microchamber. Bacterial cultures were maintained under static condition for 2 hours to allow *P. aeruginosa* PAO1 cell attachment onto the glass substrate of the microchamber. Attached bacteria were exposed to flowing media at 0.2 μl/min for 72 hours.

Integration of confocal micro-Raman spectroscopy with microfluidic platform.

A confocal micro-Raman spectroscopic system (Renishaw, Gloucestershire, UK) with 532 nm green diode laser was applied for the characterization of chemical compositions and formation level of *P. aeruginosa* biofilms. Raman spectrometer is equipped with a 1200-line/mm grating. Laser light (0.2 mW laser power on sample) was introduced through a 50× objective (Leica Biosystems, Wetzlar, Germany) into the microchamber and focused on the biofilm during its formation while Raman signal was collected and dispersed by a diffraction grating, and finally recorded by using a 578- by 385-pixel charge-coupled device (CCD) array detector. Before spectral collection, Raman spectrometer was calibrated by silicon wafer for its featured Raman peak at 520 cm^{-1}. An integration time of 30 seconds was applied for spectral collection over a simultaneous Raman shift range of 1800 to 400 cm^{-1} in an extended mode. At each time point, 24 spectra were collected at random locations of a biofilm. At least three independent experiments were conducted. The Raman spectrometer was controlled via WiRE 3.4 software, which was also responsible for spectral acquisition and background correction (Renishaw, UK).

Confocal laser scanning microscope for biofilm quantification.

Confocal laser scanning microscopy (CLSM) was further applied to quantify the formation level of biofilms in the microfluidic chamber. Biofilms were stained using a Live/Dead BacLight Bacterial Viability Kit (Molecular Probes, Eugene, OR). A mixture of 1 μM of Syto-9 (green fluorescence for live cells) and 5 μM of propidium iodide (PI; red fluorescence for dead cells) was injected into the

47 microchamber at 2 µl/min between 30 minutes and 2 hours [2]. Images were then taken on a Fluoview
48 FV1000 confocal laser scanning microscope (CLSM) (Olympus, Melville, NY) with multi laser channel
49 at 488 nm (green fluorescence) and 543 nm (red fluorescence). At each time point, CLSM images were
50 collected at 8 random locations of a biofilm. At least three independent experiments were conducted.
51 Biofilm thickness, three-dimensional reconstruction and live/dead cells distribution were conducted
52 using Imaris software (Bitplane, South Windsor, CT).
53
54 **Chemometric models.**
55 Unsupervised principle component analysis (PCA) was applied to differentiate variations among
56 biofilms at different growth phases without a priori knowledge. Support vector machine (SVM) was
57 applied to cluster different sample groups according to PCA plot score [3]. *Mahalanobis* distance derived
58 from PCA model was applied to evaluate the distance between the centroids of different clusters [4].
59 Partial least-squares regression (PLSR) model was further applied to correlate biofilm formation
60 determined by Raman spectroscopy and CLSM. Both PCA and PLSR model were constructed in Matlab
61 (Mathworks, USA).
62
63

Table S1 Raman band assignments of *P. aeruginosa* biofilm grown in a microfluidic "lab-on-a-chip" platform [5-11].

Peaks (cm^{-1})	Assignment			
	Nucleic acids	Proteins	Lipids	Carbohydrates
746	T ring *str*	Cytochrome c		
918		Proline; hydroxyproline		Glycogen
968			Lipids	
1123		C-C *str*; cytochrome c	C-N, C-C *str*	C-C str, C-O-C glycosidic link; ring breath, *sym*
1167		C-C *str*		
1223		Amide III		
1307		CH_3/CH_2 *bend*; cytochrome c	CH_3/CH_2 *bend*	
1333		δ(CH)		δ(CH)
1357	G ring *str*			
1580	G, A ring *str*	Cytochrome c		

Abbreviations. *Bend*: bending, *breath*: breathing, *def*: *deformation*, *scis*: scissoring, *str*: stretching, *asym*: asymmetric, *sym*: symmetric.

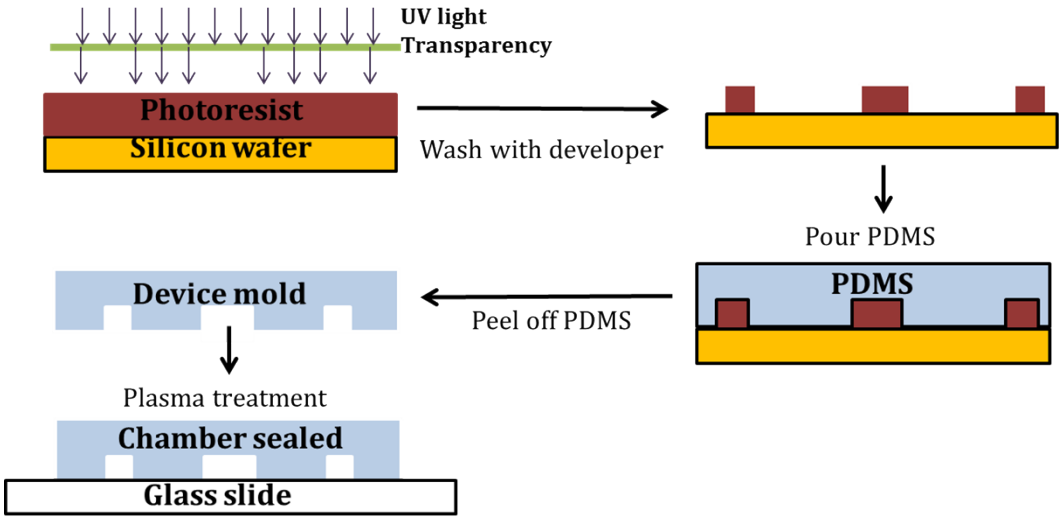

Fig. S1 Schematic procedures of soft lithography to fabricate microfluidic chip.

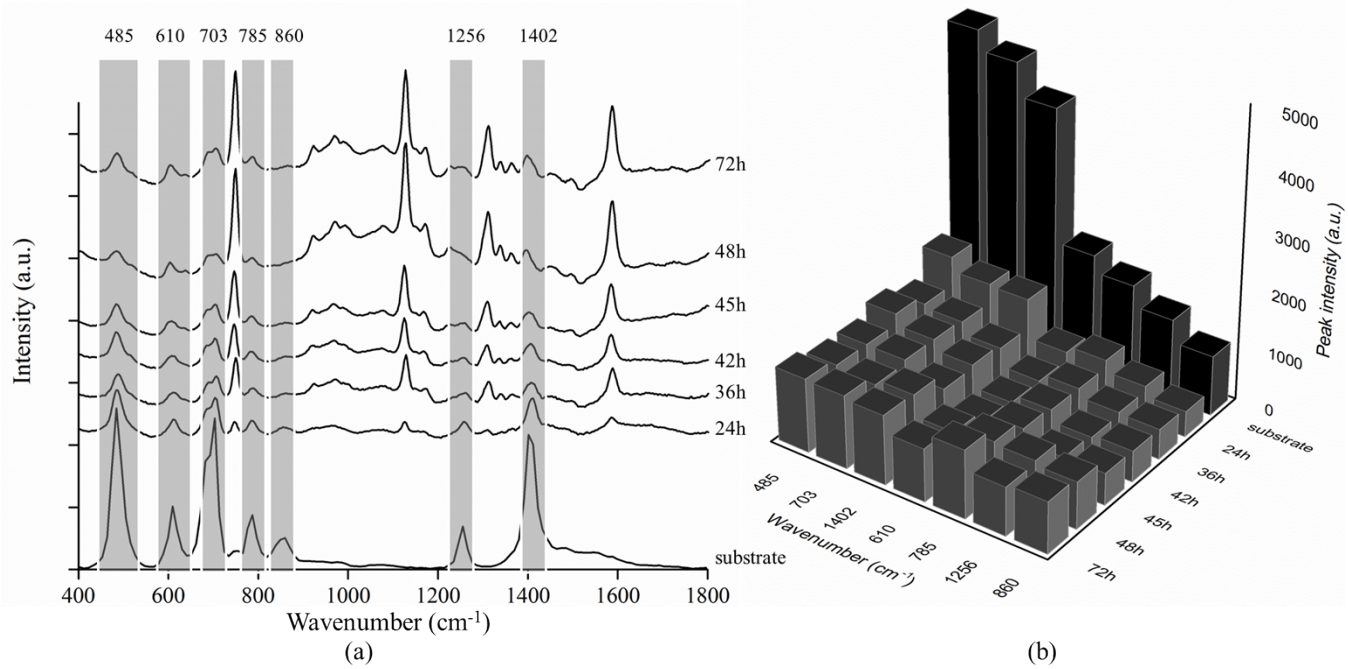

Fig. S2 Raman spectroscopy determines microfluidic chip substrate as background for biofilm characterization. (a) Prominent peaks in Raman spectra of substrate and *P. aeruginosa* biofilm grown in the microchamber; (b) Variations in Raman intensities of the corresponding peaks (485, 610, 703, 785, 860, 1256, and 1402 cm^{-1}). Shadow regions highlight variations in peak intensities of microfluidic chip substrate (as background) during *P. aeruginosa* biofilm development.

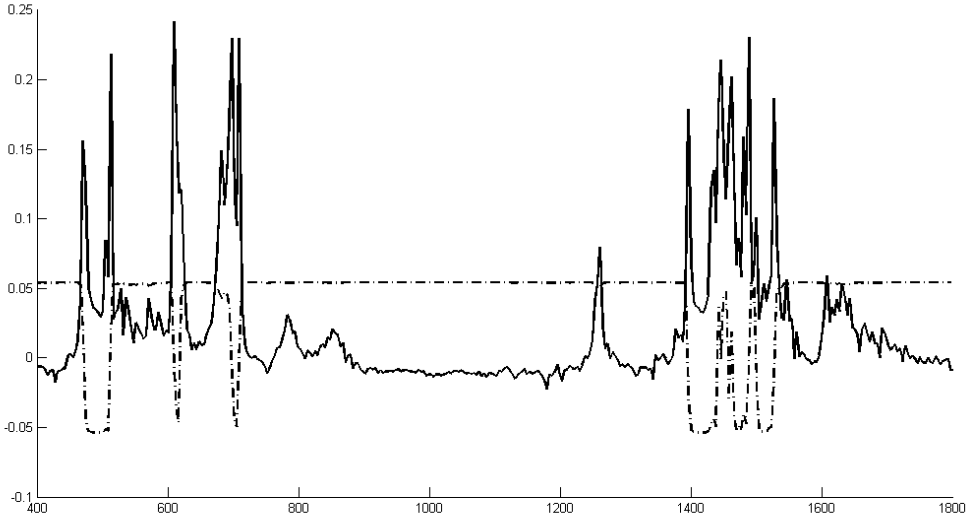

Fig. S3 Loading profile of principal component analysis. Dash line is the plot of PC1 and solid line is the plot of PC2. Absolute values of peaks represent the contribution in each component.

Supplementary references

1. D. Qin, Y. Xia and G. M. Whitesides, *Nature Protocols*, 2010, **5**, 491-502.
2. C. de la Fuente-Núñez, F. Reffuveille, E. F. Haney, S. K. Straus and R. E. Hancock, *PLoS Pathogens*, 2014, **10**, e1004152.
3. P. Rösch, M. Harz, M. Schmitt, K.-D. Peschke, O. Ronneberger, H. Burkhardt, H.-W. Motzkus, M. Lankers, S. Hofer and H. Thiele, *Applied and Environmental Microbiology*, 2005, **71**, 1626-1637.
4. X. Lu, Q. Liu, J. A. Benavides-Montano, A. V. Nicola, D. E. Aston, B. A. Rasco and H. C. Aguilar, *Journal of Virology*, 2013, **87**, 3130-3142.
5. J. De Gelder, K. De Gussem, P. Vandenabeele and L. Moens, *Journal of Raman Spectroscopy*, 2007, **38**, 1133-1147.
6. N. P. Ivleva, M. Wagner, H. Horn, R. Niessner and C. Haisch, *Analytical and Bioanalytical Chemistry*, 2009, **393**, 197-206.
7. X. Lu, A. T. Weakley, D. E. Aston, B. A. Rasco, S. Wang and M. E. Konkel, *Journal of Applied Microbiology*, 2012, **113**, 952-963.
8. M. Tang, G. D. McEwen, Y. Wu, C. D. Miller and A. Zhou, *Analytical and Bioanalytical Chemistry*, 2013, **405**, 1577-1591.
9. Z. Movasaghi, S. Rehman and I. U. Rehman, *Applied Spectroscopy Reviews*, 2007, **42**, 493-541.
10. M. Okada, N. I. Smith, A. F. Palonpon, H. Endo, S. Kawata, M. Sodeoka and K. Fujita, *Proceedings of the National Academy of Sciences*, 2012, **109**, 28-32.
11. D. S. Read, D. J. Woodcock, N. J. Strachan, K. J. Forbes, F. M. Colles, M. C. Maiden, F. Clifton-Hadley, A. Ridley, A. Vidal and J. Rodgers, *Applied and Environmental Microbiology*, 2013, **79**, 965-973.